PHYSICAL REVIEW A VOLUME 27, NUMBER 5 MAY 1983

Dependence of tagged-particle motion on size and mass

A. J. Masters and T. Keyes
Sterling Chemistry Laboratory, Yale University, New Haven, Connecticut 06520

(Received 1 September 1982)

Tagged-particle motion in fluids is studied as a function of size and mass via variational solutions of the repeated-ring and self-consistent repeated-ring equations. For a massive particle, the transition from Boltzmann to Stokes-Einstein behavior is found as the particle radius varies from small to large with respect to the mean free path. New and more complicated effects are found for light particles. The theory appears to provide an explanation of the results of the computer simulation of Alder and Alley on size and mass dependence.

I. INTRODUCTION

The nature of tagged-particle motion in fluids is determined by the collision radius (a_1) and mass (m_1) of the tagged particle, and by the density ρ of the bath. The mass enters as the ratio m_1/m of tagged-particle to bath-particle masses. The radius may either appear as a_1/a, a being the collision radius for two path particles, or mixed with the density via the Knudsen number $K_n \equiv l(\rho)/a_1$, where l is the mean free path.

If $K_n \gg 1$ and the reduced density $\rho a^3 \equiv \rho^*$ is much less than unity, the motion is well described by the Lorentz-Boltzmann equation. More interesting and difficult problems may be generated in two ways. First, a bath fluid of liquid density might be considered; no satisfactory kinetic theory exists here for any type of tagged particle. Less complicated is the case where the bath is kept dilute, but the Knudsen number is made small and the Lorentz-Boltzmann equation fails.

Even for this second situation, a good kinetic description has long been unavailable. It is now clear, however, that the repeated-ring approximation[1,2] (RRA) might provide that desired description. It correctly[3–5] gives the Stokes-Einstein law for the self-diffusion constant D in the "Brownian limit" $m_1/m \gg 1$, when $K_n \ll 1$, and it also[5,6] appears to constitute the high-mass limit of the Bogoliubov-Born-Green-Kirkwood-Yvon hierarchy. An extended, "self-consistent" RRA (SCRRA) turns out, without rigorous justification, to be remarkably useful for light particles as well. We proposed[7] and studied, for dimension (d) of 1, 2, and 3, the SCRRA for the Lorentz gas, where a point particle moves in an array of fixed overlapping "d spheres" of arbitrary density (a "real" bath will act like the fixed scatterers in the Lorentz gas if $m_1/m \ll 1$ and $\rho l a_1^2 \gg m_1/m$). The high-density regime is more tractable here than in a true liquid due to the trivial statistics of overlapping d-spheres. At a critical density of scatterers, the tagged particle becomes trapped in the Lorentz gas, and the self-diffusion coefficient D must vanish. We found that the SCRRA gave a good theory of the trapping phenomena.

The empirical success of the SCRRA for the light point particles of the Lorentz gas, coupled with its solid justification for heavy, large Brownian particles in a dilute gas, suggests that it might provide a good theory for the motion of a tagged particle of arbitrary size and mass in a dilute gas. This speculation forms the basis of the research to be reported here. Our goals are twofold. First, even given a situation where the SCRRA is believed valid, the equation must be solved, which is a major task. In a recent paper,[8] we showed how the variational principle of Cercignani[9,10] developed for the calculation of drag on objects in flowing gases, could, when combined with a Bhatnagar-Gross-Krook[11] (BGK) approximation, be used to numerically solve the RRA. We applied the method to the Lorentz gas for the RRA[8] and SCRRA,[7] obtaining what appeared to be solutions of great accuracy. So, our first objective is to set up the variational method to solve both the RRA and the SCRRA for a tagged particle in a real gas.

Second, we want to obtain a qualitative and a quantitative understanding of the size and mass dependence of D, in a dilute gas, for all m_1 and a_1. In the Brownian case, we obtain D as a function of K_n for the full range of K_n, from $K_n \gg 1$ to $K_n \ll 1$; D varies smoothly from its Lorentz-Boltzmann to its Stokes-Einstein value. Our calculation is closely related to various empirical and theoretical attempts to find the drag on fixed objects for all K_n, insofar as D and the drag are interrelated by Einstein's law for a massive particle. Nonetheless, it is the first *direct* calculation of $D(K_n)$ of which we are aware.

Far less is known, either experimentally or from computer simulation, about the motion of light particles in dilute gases. Here we find much more striking and unusual behavior than the smooth transition from low-density to continuum behavior for a Brownian particle. We have only been able to compare our results with the limited data of Alder *et al.*,[12] which are taken at a gas density where the RRA is unjustified; the theory is qualitatively in agreement. Further simulation studies in this area would be valuable. In addition to the SCRRA, our calculations employ a BGK approximation, the validity of which may be questioned. This is discussed at several points in the following sections.

II. REPEATED-RING EQUATIONS AND LIMITING SOLUTIONS

For most values of the key parameters, the SCRRA reduces to the RRA. Thus we introduce the RRA first, turning to the full SCRRA only when we need it later on. Let us write the Laplace-transformed velocity correlation of the tagged particle $C(z)$ in the form

$$C(z)=\int_0^\infty dt\, e^{-zt}\langle \vec{v}_1\cdot\vec{v}_1(-t)\rangle = \int d\vec{v}_1\vec{v}_1\cdot\vec{\Phi}(\vec{v}_1,z)\ , \tag{1}$$

where the angular brackets denote a canonical-ensemble average. The diffusion constant D is given in three dimensions by

$$D=\tfrac{1}{3}C(0)\ . \tag{2}$$

We now write the RRA equations[2] for $\vec{\Phi}(\vec{v}_1,z)$ in the form

$$[z-\rho\lambda_D(\vec{v}_1)]\vec{\Phi}(1) - \rho\int d\vec{r}_1 d\vec{v}_2 T(12)\vec{\theta}(12)=\vec{v}_1\phi_0(v_1) \tag{3a}$$

and

$$[z+\vec{v}_1\cdot\vec{\nabla}_1+\vec{v}_2\cdot\vec{\nabla}_2-\rho\lambda_B(\vec{v}_2)-\rho\lambda_D(\vec{v}_1)-\bar{T}(12)]\vec{\theta}(12)=T(12)\vec{\Phi}(1)\phi_0(v_2)\ . \tag{3b}$$

Here, for shorthand, we have written $\vec{\Phi}(\vec{v}_1,z)$ as $\vec{\Phi}(1)$ and $\vec{\theta}(12)$ represents $\vec{\theta}(\vec{r}_{12},\vec{v}_1,\vec{v}_2,z)$. In this equation $\vec{v}_1$ and $\vec{r}_1$ are the velocity and position vectors of the tagged particle, $\vec{v}_2$ and $\vec{r}_2$ the velocity and position vectors of a generic gas molecule, denoted as particle 2, and $\vec{r}_{12}=\vec{r}_1-\vec{r}_2$. The functions $\phi_0(v_1)$ and $\phi_0(v_2)$ are the Maxwellian velocity distribution functions of particles 1 and 2, respectively. The binary-collision operators $T(ij)$ and $\bar{T}(ij)$ describing elastic, specular hard-sphere collisions, are given by[13]

$$T(ij)=a_{ij}^2\int_{\vec{v}_{ij}\cdot\hat{\sigma}>0} d\hat{\sigma}\,|\vec{v}_{ij}\cdot\hat{\sigma}|\,\delta(\vec{r}_{ij}-a_{ij}\hat{\sigma})[\hat{b}(ij)-1] \tag{4a}$$

and

$$\bar{T}(ij)=a_{ij}^2\int_{\vec{v}_{ij}\cdot\hat{\sigma}>0} d\hat{\sigma}\,|\vec{v}_{ij}\cdot\hat{\sigma}|\,[\delta(\vec{r}_{ij}-a_{ij}\hat{\sigma})\hat{b}(ij) -\delta(\vec{r}_{ij}+a_{ij}\sigma)]\ , \tag{4b}$$

where $\vec{v}_{ij}=\vec{v}_i-\vec{v}_j$, and the operator $\hat{b}(i,j)$ transforms the postcollision velocities $\vec{v}_i$ and $\vec{v}_j$ into the precollision velocities $\vec{v}\,'_i$ and $\vec{v}\,'_j$, where

$$\vec{v}\,'_i=\vec{v}_i-(2\mu_{ij}/m_i)\hat{\sigma}(\hat{\sigma}\cdot\vec{v}_{ij}) \tag{5a}$$

and

$$\vec{v}\,'_j=\vec{v}_j+(2\mu_{ij}/m_j)\hat{\sigma}(\hat{\sigma}\cdot\vec{v}_{ij})\ . \tag{5b}$$

In these definitions, a_{ij} is the collision radius of particles i and j, which equals a when i and j are both gas particles and equals a_1 for a tagged-particle—gas-particle collision. $\hat{\sigma}$ is the unit vector joining the center of particle i to particle j, m_i is the mass of particle i and is given by m_1 for $i=1$ and m for $i\neq 1$, and μ_{ij} is the reduced mass of the colliding particles which is denoted by μ if (i,j) contains the tagged particle and is equal to $m/2$ otherwise. Finally, $\lambda_D(\vec{v}_1)$ is the Lorentz-Boltzmann operator given by

$$\lambda_D(\vec{v}_1)=\int d\vec{r}_2 d\vec{v}_2 T(12)\phi_0(v_2)\ , \tag{6a}$$

and $\lambda_B(\vec{v}_2)$ is the Boltzmann operator, given by

$$\lambda_B(\vec{v}_2)=\int d\vec{r}_3 d\vec{v}_3 T(23)(1+P_{23})\phi_0(v_3), \tag{6b}$$

where P_{23} interchanges the velocities $\vec{v}_2$ and $\vec{v}_3$. We note also that $\vec{\theta}(12)$ is zero for $|\vec{r}_{12}|<a_1$. For a full account of the derivation of these equations and the collision sequences that are taken into account, we refer to Ref. 2.

For a small particle ($a_1/l \ll 1$), Eq. (3a) reduces to the Lorentz-Boltzmann equation, given by

$$[z-\rho\lambda_D(\vec{v}_1)]\vec{\Phi}(1)=\vec{v}_1\phi_0(v_1)\ . \tag{7}$$

This gives rise to a velocity correlation function (VCF) that decays away approximately exponentially in time, provided m_1/m is not too small. At zero frequency, we may write $\vec{\Phi}(1)$ in the form

$$\vec{\Phi}(1)=\vec{v}_1 C(v_1^2)\phi_0(v_1)\ . \tag{8}$$

The diffusion constant D_{LB} may be written in the form

$$D_{\mathrm{LB}}=(k_B T/m_1)/\nu_D \ , \tag{9}$$

where T is the absolute temperature, k_B is Boltzmann's constant, and ν_D the Lorentz-Boltzmann friction coefficient, given by[14,15]

$$\nu_D=\frac{8\rho a_1^2}{3m_1}(2\pi\mu k_B T)^{1/2} f(m_1/m) \ . \tag{10}$$

The function $f(m_1/m)$ is approximately unity except for small values of m_1/m and is tabulated for many values of m_1/m by Lindenfeld.[16]

For a large and massive Brownian particle ($a_1/l \gg 1$ and $m_1/m \gg 1$, but with $\rho l a_1^2 \ll m_1/m$), we may obtain the VCF by finding the hydrodynamic solution of Eqs. (3a) and (3b). As this has been discussed in much detail elsewhere[3-5] the treatment given here will be very brief, following along the lines of the first section of Ref. 3(b). Firstly, we rewrite $\vec{\theta}(12)$ as $W(12)\vec{\theta}(12)$, where $W(12)=0$, $|\vec{r}_{12}|<a_1$ and $W(12)=1$, $|\vec{r}_{12}|\geq a_1$, and $\vec{\theta}(12)$ is now continuous. Equation (3b) may then be written in the form

$$W(12)[z+\vec{v}_1\cdot\vec{\nabla}_1+\vec{v}_2\cdot\vec{\nabla}_2-\rho\lambda_B(\vec{v}_2)-\rho\lambda_D(\vec{v}_1)]\vec{\theta}(12)=0 \tag{11a}$$

with boundary conditions at $|\vec{r}_{12}|=a_1$ given by

$$\vec{\theta}(12)+\vec{\Phi}(1)\phi_0(v_2)=\hat{b}(12)[\vec{\theta}(12)+\vec{\Phi}(1)\phi_0(v_2)] \ . \tag{11b}$$

Equation (11b) may now be used to rewrite Eq. (3a) in the form

$$z\vec{\Phi}(1)-\rho\int d\vec{r}_2 d\vec{v}_2 \int d\hat{\sigma}\,\delta(\vec{r}_{12}-a_1\hat{\sigma})(\vec{v}_{12}\cdot\hat{\sigma})\vec{\theta}(12)=\vec{v}_1\phi_0(v_1) \ . \tag{12}$$

If we now take the scalar product with $\vec{v}_1$ and integrate $d\vec{v}_1$, we obtain

$$zC(z)-\rho\int d\vec{v}_1 d\vec{v}_2 d\vec{r}_2 d\hat{\sigma}\,\delta(\vec{r}_{12}-a_1\hat{\sigma})(\vec{v}_{12}\cdot\hat{\sigma})\vec{v}_1\cdot\vec{\theta}(12)=3k_B T/m_1 \ . \tag{13}$$

As we are dealing with a massive particle, we expect that $|\vec{v}_1|$ is small compared with $|\vec{v}_2|$, and that $\vec{\theta}$ can be expanded,

$$\vec{\theta}(12)=\phi_0(1)\vec{\theta}^{(0)}(\vec{r}_{12},\vec{v}_2) +\phi_0(1)\vec{v}_1\cdot\overleftrightarrow{\theta}^{(1)}(\vec{r}_{12},\vec{v}_2)+\cdots \tag{13b}$$

with $\vec{\theta}^{(0)}$ and $\overleftrightarrow{\theta}^{(1)}$ of the same order in m/m_1. Substitution of this equation into Eq. (13a), followed by integration over $\vec{v}_1$, gives, due to the independence of $\vec{v}_1$ and $\vec{v}_2$, a result for $C(z)$, of order m/m_1, containing both $\vec{\theta}^{(0)}$ and $\overleftrightarrow{\theta}^{(1)}$. This would suggest that in order to obtain the high-mass limit of $C(z)$, both the high-mass limit of $\vec{\theta}$ and the first correction are required. Fortunately, this is not the case, because multiplication of Eq. (11b) by $\vec{v}_1\vec{v}_2$ and integrating $\int d\vec{v}_1 d\vec{v}_2$, allows us to rewrite Eq. (13) in the form

$$zC(z)-\rho\frac{m}{m_1}\int d\vec{v}_1 d\vec{v}_2 d\vec{r}_2 d\hat{\sigma}\,\delta(\vec{r}_{12}-a_1\hat{\sigma}) \times(\vec{v}_2\cdot\hat{\sigma})^2\hat{\sigma}\cdot\vec{\theta}(12)=\frac{3k_B T}{m_1} \tag{14}$$

to lowest order in $(m/m_1)^{1/2}$, where clearly $\vec{\theta}(12)$ is also only required to lowest order in $(m/m_1)^{1/2}$. This discussion illustrates some of the pitfalls lurking in the RRA; Eqs. (13) and (14) are both correct, but use of the high-mass θ in Eq. (13) gives the wrong hydrodynamic limit.

The hydrodynamic form of $\vec{\theta}(12)$, for small (m/m_1), is given by

$$\vec{\theta}_\alpha(12)=\phi_0(v_1)\phi_0(v_2)\{\vec{n}_\alpha(\vec{r}_{12})+(\beta m)^{1/2}[\vec{v}_{2,\beta}+B(v_2^2)(\vec{v}_{2,\beta}\vec{v}_{2,\gamma}-\tfrac{1}{3}v_2^2\delta_{\beta\gamma})\vec{\nabla}_{2\gamma}]\overleftrightarrow{U}_{\beta\alpha}(\vec{r}_{12}) +(\tfrac{2}{3})^{1/2}[(\tfrac{1}{2}\beta m v_2^2-\tfrac{3}{2})+A(v_2^2)\vec{v}_{2,\beta}\vec{\nabla}_{2,\beta}]\vec{T}_\alpha(\vec{r}_{12})\} \ , \tag{15}$$

where $\beta=(k_B T)^{-1}$, the greek subscripts denote Cartesian components, and the functions $A(v_2^2)$ and $B(v_2^2)$ are the same as those used by Van Beijeren and Dorfman[3] and are closely related to the thermal conductivity λ and shear viscosity η of the gas, respectively. The functions $\vec{n}$, $\overleftrightarrow{U}$, and $\vec{T}$ are found by substitution of Eq. (15) into Eqs. (11a) and (11b), which leads via Eq. (14) to the hydrodynamic forms for $C(z)$ and $\vec{\Phi}(1)$, including the slip Stokes-Einstein law for D. As the zero-frequency ($z=0$) results are needed in the subsequent sections, we now give a list of them:

$$D=k_B T/4\pi\eta a_1 \ , \tag{16a}$$

$$\vec{\Phi}(1)=\phi(v_1)\vec{v}_1(m_1/4\pi\eta a_1)\ , \tag{16b}$$

$$\vec{n}(\vec{r})=(1/4\pi\rho)\hat{r}/r^2\ , \tag{16c}$$

$$\overleftrightarrow{U}_{\alpha\beta}(\vec{r})=(m/\beta)^{1/2}(1/8\pi\eta)(\delta_{\alpha\beta}+\hat{r}_\alpha\hat{r}_\beta)/r\ , \tag{16d}$$

$$\vec{T}(\vec{r})=0\ . \tag{16e}$$

Here, as elsewhere, the caret denotes a unit vector.

The final limiting case that we consider is the Lorentz gas ($m_1/m, a_1/a \ll 1$) when the bath density is very large. This problem has previously been considered in a microcanonical ensemble,[8] but the extension to a canonical ensemble is straightforward. In this limit, $\vec{\theta}(12)$ is given by

$$\vec{\theta}_\alpha(12)=\phi_0(v_1)\phi_0(v_2)[1-C(v_1^2)\vec{v}_{1,\beta}\cdot\vec{\nabla}_{1,\beta}]\vec{m}_\alpha(\vec{r}_{12})\ , \tag{17}$$

where $C(v_1^2)$ is given by Eqs. (7) and (8).

The hydrodynamic results are now given for zero frequency,

$$D=3D_{\mathrm{LB}}/(2\pi\rho a_1^3)\ , \tag{18a}$$

$$\vec{\Phi}(1)=\phi_0(v_1)\vec{v}_1C(v_1^2)(3/2\pi\rho a_1^3)\ , \tag{18b}$$

and

$$\vec{m}(\vec{r})=-(3/4\pi\rho)\hat{r}/r^2\ . \tag{18c}$$

Equations (18) do not show percolation, for which the SCRRA is required.

We shall now proceed to set up the variational principle, so that we may obtain approximate solutions for the VCF away from those limiting cases. We shall use the results given in this section to guide us and to help check our approximations.

III. BGK APPROXIMATION, INTEGRAL EQUATION, AND THE VARIATIONAL PRINCIPLE

In order to make further progress, it is necessary to make simplifying approximations to the Lorentz-Boltzmann and Boltzmann operators that appear in the RRA. Following Cercignani[9,10] *et al.* and many other workers, we employ a single-relaxation-time approximation, the simplest BGK approximation. Thus we write

$$\rho\lambda_D(\vec{v}_1)f(\vec{v}_1)\simeq-\nu_D\left[f(\vec{v}_1)-\phi_0(v_1)\int d\vec{v}\,'_1 f(\vec{v}\,'_1)\right] \tag{19a}$$

and

$$\rho\lambda_B(\vec{v}_2)g(\vec{v}_2)\simeq-\nu_B\left[g(\vec{v}_2)-\phi_0(v_2)\int d\vec{v}\,'_2 g(\vec{v}\,'_2)[1+(\beta m)^{-1}\vec{v}_2\cdot\vec{v}\,'_2+\tfrac{2}{3}(\tfrac{1}{2}\beta m v_2^2-\tfrac{3}{2})(\tfrac{1}{2}\beta m v_2'^2-\tfrac{3}{2})]\right]\ . \tag{19b}$$

Here $f(\vec{v}_1)$ and $g(\vec{v}_2)$ are arbitrary functions of the velocity. These approximations make no difference to the limiting zero-frequency results discussed previously, provided we identify the function $C(v_1^2)$ with ν_D^{-1} and provided we choose ν_B so that the gas retains the correct Boltzmann value for its shear viscosity. To an excellent approximation (first Sonine polynomial approximation) ν_B is given by[14,15]

$$\nu_B=\frac{16a^2\rho}{5}\left[\frac{\pi}{\beta m}\right]^{1/2}\ . \tag{20}$$

As is well known, Eq. (19b) combined with Eq. (20) yields an incorrect value of the thermal conductivity—it comes out a factor of $\frac{3}{2}$ times the true value. It is our belief, though, that at zero frequency errors such as these in the BGK approximations are not so important, except when calculating corrections to D_{LB} for very small values of a_1/l. We defer further discussion of this to a later section.

We now further follow the procedure of Cercignani *et al.*[10] and, using Eqs. (19a) and (19b), we convert Eqs. (11a) and (11b) into an integral equation for $\vec{\theta}(12)$. The only differences between this problem and that considered by Cercignani lie in the differing boundary conditions (specular reflection as opposed to diffuse reflection) and in the fact that here both the tagged particle and the gas molecules are moving. In the limit $m_1/m\to0$, the problem reduces to the RRA approximation for the Lorentz gas, described in some detail previously. As in these other problems, for our purposes the whole function $\vec{\theta}(12)$ is not required—only certain moments of $\vec{\theta}(12)$ are needed. We therefore define the following functions:

$$\phi_0(v_2)\vec{m}(\vec{v}_2,\vec{r}_{12})=\int d\vec{v}_1\vec{\theta}(12)\ , \tag{21a}$$

$$\phi_0(v_1)\vec{n}(\vec{v}_1,\vec{r}_{12})=\int d\vec{v}_2\vec{\theta}(12)\ , \tag{21b}$$

$$\phi_0(v_1)\overleftrightarrow{U}_{\alpha\beta}(\vec{v}_1,\vec{r}_{12})=(\beta m)^{1/2}\int d\vec{v}_2\vec{v}_{2,\alpha}\vec{\theta}_\beta(12)\ , \tag{21c}$$

and

$$\phi_0(v_1)\vec{\mathrm{T}}(\vec{\mathrm{v}}_1,\vec{\mathrm{r}}_{12})=(\tfrac{2}{3})^{1/2}\int d\vec{\mathrm{v}}_2(\tfrac{1}{2}\beta m v_2^2-\tfrac{3}{2})\vec{\theta}(12)\ . \tag{21c}$$

Clearly, these functions are not completely independent. Thus they must satisfy the following equations:

$$\int d\vec{\mathrm{v}}_2\phi_0(v_2)\vec{\mathrm{m}}(\vec{\mathrm{v}}_2,\vec{\mathrm{r}})=\int d\vec{\mathrm{v}}_1\phi_0(v_1)\vec{\mathrm{n}}(\vec{\mathrm{v}}_1,\vec{\mathrm{r}})\ , \tag{22a}$$

$$(\beta m)^{1/2}\int d\vec{\mathrm{v}}_2\phi_0(v_2)\vec{\mathrm{v}}_{2,\alpha}\vec{\mathrm{m}}_\beta(\vec{\mathrm{v}}_2,\vec{\mathrm{r}})=\int d\vec{\mathrm{v}}_1\phi_0(V_1)\overleftrightarrow{U}_{\alpha\beta}(\vec{\mathrm{v}}_1,\vec{\mathrm{r}})\ , \tag{22b}$$

and

$$(\tfrac{2}{3})^{1/2}\int d\vec{\mathrm{v}}_2\phi_0(v_2)(\tfrac{1}{2}\beta m v_2^2-\tfrac{3}{2})\vec{\mathrm{m}}(\vec{\mathrm{v}}_2,\vec{\mathrm{r}})=\int d\vec{\mathrm{v}}_1\phi_0(v_1)\vec{\mathrm{T}}(\vec{\mathrm{v}}_1,\vec{\mathrm{r}})\ . \tag{22c}$$

The resulting equation for $\vec{\theta}(12)$, obtained from Eq. (11a) by integrating along the characteristic lines and then using the boundary condition, Eq. (11b), may be written in the form

$$\begin{aligned}\vec{\theta}_\alpha(12)=&-\chi(\vec{\mathrm{r}}_{12}-\vec{\mathrm{r}}_0)[\phi_0(v_2)\vec{\Phi}_\alpha(\vec{\mathrm{v}}_1,z)-\phi_0(v_2')\vec{\Phi}_\alpha(\vec{\mathrm{v}}_1,z)]\\&+\frac{\phi_0(v_1)\phi_0(v_2)}{|\vec{\mathrm{v}}_{12}|}\left[\int_c dr\,\chi(\vec{\mathrm{r}}_{12}-\vec{\mathrm{r}})[\nu_D\vec{\mathrm{m}}_\alpha(\vec{\mathrm{v}}_2,\vec{\mathrm{r}})+\nu_B\vec{\mathrm{n}}_\alpha(\vec{\mathrm{v}}_1,\vec{\mathrm{r}})+\beta m\nu_B\vec{\mathrm{v}}_{2,\beta}\overleftrightarrow{U}_{\beta\alpha}(\vec{\mathrm{v}}_1,\vec{\mathrm{r}})\right.\\&\left.\qquad+(2\nu_B/3)(\tfrac{1}{2}\beta m v_2^2-\tfrac{3}{2})\vec{\mathrm{T}}_\alpha(\vec{\mathrm{v}}_1,\vec{\mathrm{r}})]\right]\\&+\frac{\phi_0(v_1)\phi_0(v_2)\chi(\vec{\mathrm{r}}_{12}-\vec{\mathrm{r}}_0)}{|\vec{\mathrm{v}}_{12}|}\left[\int_{c'}dr'\chi(\vec{\mathrm{r}}'-\vec{\mathrm{r}}_0)[\nu_D m_\alpha(\vec{\mathrm{v}}'_2,\vec{\mathrm{r}}')\right.\\&\qquad+\nu_B\vec{\mathrm{n}}_\alpha(\vec{\mathrm{v}}'_1,\vec{\mathrm{r}}')+m\nu_B\vec{\mathrm{v}}'_{2,\beta}\cdot\overleftrightarrow{U}_{\beta\alpha}(\vec{\mathrm{v}}'_1,\vec{\mathrm{r}}')\\&\left.\qquad+(\tfrac{2}{3})^{1/2}\nu_B(\tfrac{1}{2}\beta m v_2'^2-\tfrac{3}{2})\vec{\mathrm{T}}_\alpha(\vec{\mathrm{v}}'_1\cdot\vec{\mathrm{r}}')]\right]\ ,\end{aligned} \tag{23a}$$

where

$$\chi(\vec{\mathrm{r}})=\exp[-(z+\nu_B+\nu_D)|\vec{\mathrm{r}}|/|\vec{\mathrm{v}}_{12}|]\ . \tag{23b}$$

The point $\vec{\mathrm{r}}_0$ is found as follows. In the coordinate frame where the center of particle 1 is taken as the origin, $\vec{\mathrm{r}}_0$ is that value of $\vec{\mathrm{r}}_{12}$, either at the surface of particle 1 or else at infinity, from which particle 2 must leave, so that traveling with constant velocity $-\vec{\mathrm{v}}_{12}$ it eventually reaches the point $\vec{\mathrm{r}}_{12}$. The c subscript on the first integral means that the integral should be done over the straight line joining the points $\vec{\mathrm{r}}_{12}$ and $\vec{\mathrm{r}}_0$. The c' subscript on the second integral means the path of integration is over the straight line from $\vec{\mathrm{r}}_0$ on the surface of particle 1 to infinity in the same direction as $-\vec{\mathrm{v}}'_{12}$, where $\vec{\mathrm{v}}'_{12}-\vec{\mathrm{v}}'_1-\vec{\mathrm{v}}'_2$, the primed velocities having been defined in Eqs. (5a) and (5b).

Substitution of Eq. (23a) into Eqs. (21a)–(21d) yields four coupled integral equations for the moments of $\vec{\theta}(12)$. We write these equations schematically in the form

$$f_i=\sum_j(\hat{A}_{ij}f_j)-S_i\ , \tag{24}$$

where f_i represents the moments, $\hat{A}_{ij}$ is an integral operator, and S_i is a source, involving the function $\vec{\Phi}(1)$. Thus with Eqs. (3a), (23a), and (24) we have five coupled equations for the five unknown functions, i.e., $\vec{\Phi}(1)$ and the four moments. Unfortunately, unlike the Lorentz gas in a microcanonical ensemble, the functional form of $\vec{\Phi}(1)$ is unknown.

In order to make further progress, we set up two variational principles. Firstly, we may formally solve Eq. (3b) for $\vec{\theta}(12)$ and substitute the result in Eq. (3a). The resulting equation for $\vec{\Phi}(1)$ may be written

$$[z-\rho\lambda_D(\vec{\mathrm{v}}_1)-\hat{R}(\vec{\mathrm{v}}_1)]\vec{\Phi}(1)=\vec{\mathrm{v}}_1\phi_0(v_1)\ , \tag{25a}$$

where

$$\hat{R}(\vec{\mathrm{v}}_1)\vec{\Phi}(1)=\rho\int d\vec{\mathrm{r}}_2 d\vec{\mathrm{v}}_2\bar{T}(12)\vec{\theta}(12)\ . \tag{25b}$$

We now introduce the functional J, defined by

$$J(\tilde{\vec{\Phi}}(1))=\langle\tilde{\vec{\Phi}}(1)\,|\,[z-\rho\lambda_D(\vec{v}_1)-\hat{R}(\vec{v}_1)]\vec{\Phi}(1)-2\vec{v}_1\phi_0(v_1)\rangle\ , \tag{26a}$$

where the angular brackets here denote a scalar product, defined by

$$\langle\vec{f}(\vec{v}_1)\,|\,\vec{g}(\vec{v}_1)\rangle=\int d\vec{v}_1\vec{f}(\vec{v}_1)\cdot\vec{g}(\vec{v}_1)\phi_0^{-1}(\vec{v}_1)\ , \tag{26b}$$

for arbitrary functions $\vec{f}(\vec{v}_1)$ and $\vec{g}(\vec{v}_1)$. Clearly, if we set $\tilde{\vec{\Phi}}(1)=\vec{\Phi}(1)$ in Eq. (26a), we have the result

$$J(\vec{\Phi}(1))=-C(z)\ . \tag{27}$$

Furthermore, if we write

$$\tilde{\vec{\Phi}}(1)=\vec{\Phi}(1)+\delta\vec{\Phi}(1)\ , \tag{28}$$

then substitution of this into Eq. (26a) and using the fact that both the operators $\lambda_D(\vec{v}_1)$ and $\hat{R}(\vec{v}_1)$ are symmetric yields the result

$$J(\tilde{\vec{\Phi}}(1))=-C(z)+\langle\delta\vec{\Phi}(1)\,|\,[z-\rho\lambda_D(\vec{v}_1)-R(\vec{v}_1)]\delta\vec{\Phi}(1)\rangle\ . \tag{29}$$

Thus in order to obtain an approximate value for $C(z)$, we guess a trial function $\tilde{\vec{\Phi}}(1)$ that contains a number of variable parameters. These are then varied until the functional $J(\tilde{\vec{\Phi}}(1))$ attains a stationary value. This stationary value is then equal to $-C(z)$ with an error related to the square of that in the trial function.

The only term in $J(\tilde{\vec{\Phi}}(1))$ that will prove difficult to calculate is the term $\langle\tilde{\vec{\Phi}}(1)\,|\,R(\vec{v}_1)\tilde{\vec{\Phi}}(1)\rangle$. We now show within the BGK approximations given by Eqs. (19a) and (19b) that this term is very closely related to the functions f_i and S_i. Let us introduce the function $\tilde{\vec{\theta}}(12)$, which is given by Eq. (23a) if $\vec{\Phi}(1)$ is replaced by $\tilde{\vec{\Phi}}(1)$, and let us denote the moments of $\tilde{\vec{\theta}}(12)$ by $\tilde{m}$, etc. It is then possible to show, using an obvious extension of the methods used previously[10] that

$$\begin{aligned}\langle\tilde{\vec{\Phi}}(1)\,|\,\hat{R}(\vec{v}_1)\tilde{\vec{\Phi}}(1)\rangle&=\rho\int d\vec{v}_1d\vec{v}_2d\vec{r}_2\phi_0^{-1}(v_1)\tilde{\vec{\Phi}}_\alpha(1)\bar{T}(12)\tilde{\vec{\Phi}}_\alpha(12)\\&=\rho\{\nu_D[\tilde{\vec{m}},\tilde{\vec{S}}_m]+\nu_B[\tilde{\vec{n}},\tilde{\vec{S}}_n]-\beta\nu_B[\tilde{\overleftrightarrow{U}},\tilde{\overleftrightarrow{S}}_u]+(2\nu_B/3)[\tilde{\vec{T}},\tilde{\vec{S}}_T]\}\ .\end{aligned} \tag{30}$$

In these equations $\tilde{S}_i$ is a modified source term, obtained by replacing $\vec{\Phi}(1)$ with $\tilde{\vec{\Phi}}(1)$ in the original source term S_i. The square brackets denote a new scalar product, given by

$$[\vec{h}(\vec{v}_i,\vec{r}),\vec{g}(\vec{v}_i,\vec{r})]=\int_V d\vec{r}\int d\vec{v}_i\phi_0(v_i)\vec{h}(-\vec{v}_i,\vec{r})\cdot\vec{g}(\vec{v}_i,\vec{r}) \tag{31a}$$

and

$$[\overleftrightarrow{h}(\vec{v}_i,\vec{r}),\overleftrightarrow{g}(\vec{v}_i,\vec{r})]=\int_V d\vec{r}\int d\vec{v}_i\phi_0(v_i)h_{\alpha\beta}(-\vec{v}_i,\vec{r})g_{\alpha\beta}(\vec{v}_i,\vec{r})\ , \tag{31b}$$

where V refers to the whole of space with $|\vec{r}|\geq a_1$, and h and g are arbitrary functions.

In order to obtain the right-hand side (rhs) of Eq. (30), let us introduce the new functional $K(\{\tilde{f}'_i\};\tilde{\vec{\Phi}}(1))$, defined by

$$K(\{\tilde{f}'_i\};\vec{\Phi})=\sum_{i,j}W_i[\tilde{f}'_i,\tilde{f}'_i-\hat{A}_{ij}\tilde{f}'_j+2\tilde{S}_i]\ , \tag{32}$$

where

$$W_m=\nu_D\ , \tag{33a}$$

$$W_n=\nu_B\ , \tag{33b}$$

$$W_u=-\beta m\nu_B\ , \tag{33c}$$

and

$$W_T=2\nu_B/3\ . \tag{33d}$$

If we set $\tilde{f}'_i=\tilde{f}_i$, we have

$$K(\{\tilde{f}_i\};\tilde{\Phi})=\sum_i W_i[\tilde{f}_i,\tilde{S}_i]\ , \tag{34}$$

which is exactly what is required on the rhs of Eq. (30). If we further write

$$\tilde{f}'_i=\tilde{f}_i+\delta\tilde{f}_i\ , \tag{35}$$

then we obtain the result

$$\begin{aligned}&K(\{\tilde{f}'_i\};\tilde{\Phi})\\&\quad=K(\{\tilde{f}_i\};\tilde{\Phi})+\sum_{i,j}W_i[\delta\tilde{f}_i,\delta\tilde{f}_i-\hat{A}_{ij}\delta\tilde{f}_j]\ ,\end{aligned} \tag{36}$$

where we have used the relation

$$W_i[h_i,\hat{A}_{ij}g_j]=W_j[g_j,\hat{A}_{ji}h_i] \tag{37}$$

for arbitrary functions g_i and h_i. This forms our second variational principle, very similar to that employed by Cercignani *et al.*[10] The main new feature here is that all the results are to be regarded as functionals of $\tilde{\vec{\Phi}}$, which is yet to be determined.

In order to clarify the procedure that we intend to employ, let us summarize the basic working equations. For trial functions $\tilde{\vec{\Phi}}(1)$, $\tilde{\vec{\mathrm{m}}}'(\vec{\mathrm{v}}_2,\vec{\mathrm{r}})$, $\tilde{\vec{\mathrm{n}}}'(\vec{\mathrm{v}}_1,\vec{\mathrm{r}})$, etc., we obtain the VCF from the equation

$$C(z)=-\mathrm{Stat}[J(\tilde{\vec{\Phi}}(1))] \,, \tag{38}$$

where

$$\begin{aligned}J(\tilde{\vec{\Phi}}(1))=&(z+\nu_D)\langle\tilde{\vec{\Phi}}(1)\,|\,\tilde{\vec{\Phi}}(1)\rangle\\&-2\langle\tilde{\vec{\Phi}}(1)\,|\,\vec{\mathrm{v}}_1\phi_0(v_1)\rangle\\&-\rho\,\mathrm{Stat}[K(\{\tilde{f}'_i\};\tilde{\vec{\Phi}}(1))] \,.\end{aligned} \tag{39}$$

Stat*J* and Stat*K* mean the stationary values of the functionals J and K, respectively. For further insight, let us choose the trial function $\tilde{\vec{\Phi}}(1)$ to be of the form

$$\tilde{\vec{\Phi}}(1)=\alpha\vec{\mathrm{v}}_1\phi_0(v_1) \,, \tag{40}$$

where α is a parameter to be varied. This choice is the form of the exact $\vec{\Phi}(1)$ in all of the limiting cases discussed in Sec. II. Furthermore, for a sufficiently massive tagged particle of any size, we expect the exact $\vec{\Phi}(1)$ to be of the form given in Eq. (40). Thus we believe Eq. (40) to be an excellent choice for a trial function, becoming exact in several limits. If we express $C(z)$ in the form

$$C(z)=\frac{(3k_BT/m_1)}{z+\nu(z)} \,, \tag{41}$$

we obtain from Eqs. (38)—(40) the result

$$\nu(z)\simeq\nu_D-\frac{\beta m_1\rho}{3}\mathrm{Stat}[K(\{\tilde{f}'_1\};\vec{\mathrm{v}}_1\phi_0(v_1))] \,. \tag{42}$$

Optimization of α has been easy due to the linearity of S, and thus f', with Φ; note that α no longer enters K, so Stat*K* may now be found in a straightforward manner. The true value of Stat$K(\{\tilde{f}'_i\};$ $v_1\phi_0(v_1))$ is attained when $\tilde{f}'_i=\tilde{f}_i$, where $\tilde{f}_i$ is the solution of Eq. (24) with $\vec{\Phi}(1)$ replaced by $\vec{\mathrm{v}}_1\phi_0(v_1)$ in the source terms. We then may express Eq. (42) as

$$\begin{aligned}\nu(z)=\nu_D-\frac{\beta m_1\rho}{3}\{&\nu_D[\tilde{\vec{\mathrm{m}}},\tilde{\vec{\mathrm{S}}}_m]+\nu_B[\tilde{\vec{\mathrm{n}}},\tilde{\vec{\mathrm{S}}}_n]\\&-\beta m\nu_B[\tilde{\overleftrightarrow{U}},\tilde{\overleftrightarrow{S}}_u]\\&+(2\nu_B/3)[\tilde{\vec{\mathrm{T}}},\tilde{\vec{\mathrm{S}}}_T]\} \,,\end{aligned} \tag{43}$$

where $\tilde{S}_i$ is the modified source term. We may now regard the first term in the curly brackets as being a diffusive contribution towards $\nu(z)$, the second term as corresponding to a contribution from fluid density fluctuations, the third as a contribution from the fluid velocity field, and the fourth as arising from temperature fluctuations in the fluid. In the Lorentz-gas limit only the diffusive mode contributes. On the other hand, in the Brownian particle limit, when $\nu(z)$ becomes equal to the drag coefficient, the diffusive mode is negligible, the number density and temperature modes combined correspond to the pressure contribution to the hydrodynamic drag, and the Boltzmann friction coefficient and the velocity mode combined correspond to that part of the hydrodynamic drag directly caused by the fluid's velocity field.

With the choice of trial function $\tilde{\vec{\Phi}}(1)$ as in Eq. (40), Eq. (42) becomes the basic working equation and is exact when $m_1/m\gg1$. In order to obtain a breakdown of the various contributions to $\nu(z)$ when we do not know the exact form of the moments, we choose trial functions $\tilde{f}'_i$ and find their values such that K becomes stationary. It is then easily shown that the variational principle's approximate value for $\nu(z)$ is given by Eq. (43) when the exact moments $\tilde{f}_i$ in the expressions are replaced by the optimized values of the trial functions $\tilde{f}'_i$.

In summary, then, Eqs. (38) and (39) are the main results of this analysis. We expect them to yield a VCF which has an error related to the squares of the errors of the trial functions. Thus, in our opinion, we expect that these variational methods constitute numerically accurate and convenient ways of obtaining solutions, given the BGK approximations, to the RRA kinetic equations.

IV. NUMERICAL RESULTS AND DISCUSSION

Although the variational method allows us, in principle, to calculate the time-dependent VCF from the RRA, we shall simply concentrate upon the diffusion constant here. We choose the trial function $\tilde{\vec{\Phi}}(1)$ to be given by Eq. (40). As for the trial functions for the moments required in Eq. (39), we follow Cercignani[10] and pick them to be proportional to the hydrodynamic forms listed in Sec. II. Thus we take

$$\tilde{\vec{\mathrm{n}}}'(\vec{\mathrm{v}}_1,\vec{\mathrm{r}})=b_1\hat{r}/r^2 \,, \tag{44a}$$

$$\tilde{\overleftrightarrow{U}}'(\vec{\mathrm{v}}_1,\vec{\mathrm{r}})=b_2(\delta_{\alpha\beta}+\hat{r}_\alpha\hat{r}_\beta)/r \,, \tag{44b}$$

$$\tilde{\vec{\mathrm{T}}}'(\vec{\mathrm{v}}_1,\vec{\mathrm{r}})=b_3\hat{r}/r^2 \,, \tag{44c}$$

and

$$\tilde{\vec{m}}'_\alpha(\vec{v}_2,\vec{r})=\tilde{\vec{n}}'_\alpha(\vec{0},\vec{r})+\beta m\vec{v}_{2,\gamma}\cdot\tilde{\overleftrightarrow{U}}'_{\gamma\alpha}(\vec{0},\vec{r})$$
$$+\tfrac{2}{3}(\tfrac{1}{2}\beta m v_2^2-\tfrac{3}{2})\tilde{\vec{T}}'_\alpha(\vec{0},\vec{r})\ , \qquad (44d)$$

where b_1, b_2, and b_3 may be varied. The choice of the functional form of $\vec{T}'(\vec{v}_1,\vec{r})$ was motivated by the fact that this would have been the form obtained from the hydrodynamic solution in the Brownian particle limit had not the boundary conditions forced the coefficient b_3 to be zero. Away from this limit, though, there is no reason to expect this term to vanish. The choice of $\vec{m}'$ ensures that the equalities given in Eqs. (22a)—(23c) are satisfied.

As a check upon our working, we actually used the variational principle to calculate the coefficients b_1, b_2, and b_3 in these known limits. As expected, they came out to be the same as listed previously. Away from these limits, though, the integrals required to find these coefficients were done numerically. The gas parameters used in most of the calculation were taken to roughly resemble argon at standard temperature and pressure. The figures used were

$$\rho l^3=500\ , \qquad (45a)$$

where l is given by

$$l^{-1}=4\pi\rho a^2\ . \qquad (45b)$$

These equations show that $a/l=0.013$, so that the gas would, in reality, obey the Boltzmann equation fairly accurately; these are conditions where the RRA should be valid for a massive particle.

For a very massive particle ($m_1/m=10^{10}$), we plot v/v_D [where $v=v(z=0)$] against a_1/l, that is, K_n^{-1}. This is shown in Fig. 1. Using Eq. (43), we have also shown on the figure the contributions from the number density and temperature modes, and from the negative of the velocity mode. The "total" curve shows a monotonic decrease with increasing size of particle. This result is qualitatively similar to Cercignani's results and to the empirical interpolations for the drag on a sphere, though, as discussed earlier, we are considering only a specular reflecting sphere here. It is also clear from the figure that the contribution of the temperature mode to the total is very small. If, however, one is interested in the deviation of v/v_D from unity, then at very small values of a_1/l, the temperature mode does make a significant percentage contribution to that extremely small deviation. Now, as we discussed earlier, the BGK approximation to the Boltzmann operator, Eq. (19b), gives the gas an incorrect thermal conductivity, and one would imagine that the thermal conductivity would be more intimately connected to the temperature mode than any other. Thus as the contribution of the temperature mode is negligible for all except the smallest values of a_1/l, we expect that this shortcoming of the BGK approximation is not too important. When the temperature mode is important in determining v/v_D we believe the BGK approximation to be inadequate. As a general rule, we do not put much faith in the numerical predictions of the variational principle when the temperature mode does turn out to be of importance.

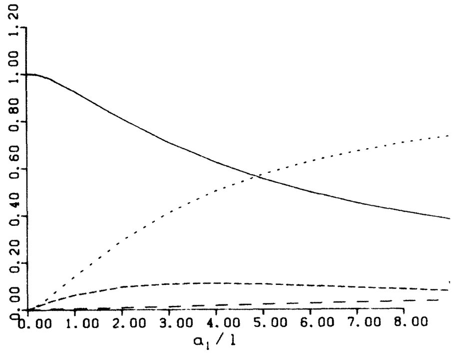

FIG. 1. Solid line is v/v_D vs a_1/l for "Brownian" particle $m_1/m=10^{10}$. Dashed lines give the negative of the contribution to $(v/v_D)-1$ of the velocity mode (small dashes), and the contributions of the density (medium size dashes) and temperature (large dashes) modes.

We may analyze the predictions of the RRA and BGK approximations more thoroughly at low values of a_1/l. As discussed previously, for $m_1/m \gg 1$, Eq. (43) becomes exact. Furthermore, when $a_1/l \ll 1$, we have

$$\tilde{f}_i=\tilde{S}_i[1+O(a_1/l)]\ . \qquad (46)$$

Thus within the BGK approximation and for high-mass ratio, it is easy to exactly calculate the first-order correction to v_D in powers of a_1/l. The numerical results are

$$v=v_D+\frac{m\rho a_1^3 v_B}{m_1}(3.669-4.165+0.612) \qquad (47a)$$

or

$$v=v_D+\frac{m\rho a_1^3 v_B}{m_1}\times 0.116\ . \qquad (47b)$$

The three numbers in the parentheses of Eq. (47a) are the contributions, reading from left to right, of the number density, velocity, and temperature modes, respectively. Clearly, there is an extensive cancellation occurring to give the final result in Eq. (47b), the magnitude of the sum being considerably less than any of the individual contributions. Thus as the BGK model employed here treats the temperature mode incorrectly and also as Eq. (47a) suggests that great cancellations are taking place, it seems probable that a model operator with a very large number of relaxation times will be required to obtain an accurate first-order correction term. We therefore conclude that for small a_1/l our curves are untrustworthy due largely to the inadequacy of our BGK approximations, but that for larger a_1/l the insignificance of the temperature mode suggests the curves are going to be more accurate. We note also that we repeated the variational calculation, setting $\overset{\leftrightarrow}{\mathrm{T}}'(\vec{\mathrm{v}}_1,\vec{\mathrm{r}})$ to be zero. Except for very small a_1/l, the curve obtained was identical, to 1 part in 10^3, to that shown in the figure.

As mentioned above, considerable effort has been expended in obtaining the drag for $a_1/l \simeq 1$, the "transition regime"; one reason for studying the drag is to find D. Almost all previous work, however, has been for objects with "stick," or "diffuse reflection" boundary calculations. Our results should give a good characterization of the transition behavior where slip, or specular reflection, is appropriate.

In Figs. 2–4, we plot ν/ν_D against particle size for differing mass ratios at the same low gas density. Again, the fact that in all these curves, changing the trial function $\overset{\leftrightarrow}{\mathrm{T}}'(\vec{\mathrm{v}}_1,\vec{\mathrm{r}})$ from the expression given in Eq. (44c) to zero made less than 1% difference to the final curve, suggests that again the BGK approximation is generally working well. In Fig. 2, we compare the plots for $m_1/m = 10^{10}$, 10^4, and 2×10^2, respectively. Clearly, the curves die away faster the lower the mass ratio is, but they all show a monotonic decrease with increasing size of particle, except for a tiny and probably spurious maximum at very low a_1/l due to the effects discussed above. In Fig. 3, where m_1 and m are equal, the plot exhibits a marked initial increase, a maximum, and then a decay. In Fig. 4, where $m_1/m = 10^{-2}$ the maximum is still more pronounced. We do not believe that these maxima are spurious, for the effects of the temperature mode are negligible. As m_1/m becomes smaller, the position of the maximum moves in slightly towards smaller a_1/a, and its height increases.

In order to get some insight into this kind of behavior, let us consider the Lorentz-gas limit $m_1/m \rightarrow 0$ in this RRA approximation. From our previous study,[8] we know that on this limit ν/ν_D is a monotonically increasing function as a_1 increases. The fact that for finite m_1/m the curves eventually start to decrease again after a certain value of a_1/a is evidently somehow associated with the motion of the fluid molecules. The figures from the mode analysis, Eq. (43), show that the initial rise is caused by the first term on the rhs of Eq. (44d) for $\overset{\leftrightarrow}{\mathrm{m}}'(\vec{\mathrm{v}}_2,\vec{\mathrm{r}})$—a purely diffusive term. For larger particles, however, the negative contribution of the second term on the rhs of Eq. (44d) outweighs the first and causes the eventual decrease. As this second term explicitly involves the motion of the fluid particles, one is tempted to interpret the final, total curve as initially representing the motion of the tagged particle in a static lattice and the eventual decrease as being associated with the disruption of this lattice due to fluid motion. Insofar as the velocity mode of the fluid dominates at large a_1, we may be seeing a "mode-coupling" effect associated with fluctuating convective diffusion, but we do not currently have a detailed understanding of this point.

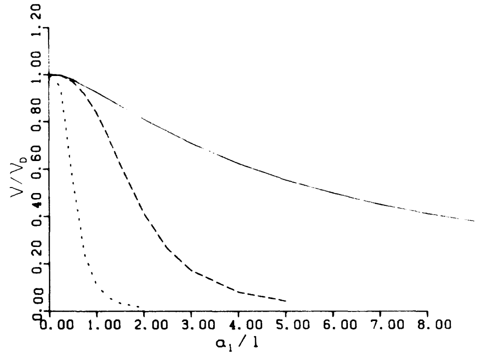

FIG. 2. Plot of ν/ν_D vs a_1/l for mass ratios of 10^{10} (solid line), 10^4 (large dashes), and 2×10^2 (small dashes).

The behavior of ν/ν_D for light particles is intriguing, and we would like to compare our results with computer simulation or experiment. Unfortunately, the only relevant simulation of which we are aware, that of Alder *et al.*,[12] probes fluid densities where the bath cannot be expected to obey the Boltzmann equation, and thus the RRA is of dubious value. More importantly, when ν/ν_D is very large, as can

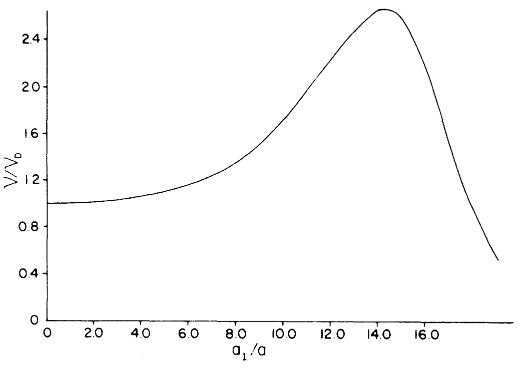

FIG. 3. Plot of ν/ν_D vs a_1/a for unit mass ratio.

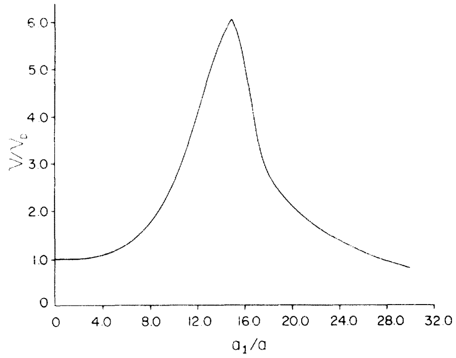

FIG. 4. Plot of v/v_D vs a_1/a for mass ratio of 10^{-2}.

be the case for light particles, the system is Lorentz-gas-like, and we believe that the SCRRA must be used. We consider these points in Sec. V.

We finish this section by considering possible errors in our methods and possible improvements that could be made. Given the RRA equations, the approximations are of two kinds. Firstly, there are the BGK approximations. Secondly, there is the question of how accurate the variational procedure is. Taking the BGK question first, the systematic thing to do would be to improve the model by introducing more than one relaxation time, set up the variational principle for this new model, and investigate whether the final results change. As we argued earlier, it is our belief that the single-relaxation-time model is good for the diffusion constant provided that we are not considering corrections to D_B at low a_1/l, but strictly speaking this requires more proof. Also, as stressed by Lindenfeld,[16] the BGK model for $\lambda_D(v_1)$ does not give an accurate time-dependent VCF when $m_1/m \ll 1$, and $a_1/l \ll 1$, but so long as we are only calculating diffusion constants, this may not be an important correction. The BGK model used here yields the correct low-density diffusion constant for all m_1/m.

The question of the accuracy of the variational principles is harder to answer. One problem with the principles here is that one requires only the stationary value of the functional, as opposed to a maximum or a minimum. Thus it has proved impossible, at least so far, to put bounds upon the error one has made. In practice, though, we believe that this deficiency is probably not too important. The limiting, hydrodynamic solutions allow us to choose sensible trial functions and, furthermore, Cercignani[9,10] has shown how their variational approach gives extremely accurate results for a wide range of problems. He also showed, as we did for the Lorentz gas,[8] that using more flexible trial functions made negligible difference to the final answer. In the study presented here, we have not conducted this check, except as to whether including a temperature mode or not alters anything. Clearly, this would be another possible way of improving the calculation.

In conclusion, we believe that the results presented are accurate, but further work should be done to check the validity of the BGK approximation and whether the quality of the trial functions used was high enough. To this extent, the results here must be regarded as the first step towards a really good solution. it is our belief, though, that in spite of the deficiencies already discussed, that the method proposed here is an attractive and powerful means of obtaining accurate solutions to the RRA.

V. SELF-CONSISTENT RRA AND NUMERICAL RESULTS

The normal RRA equations, when applied to the Lorentz gas with overlapping scatterers, predicts [Eqs. (18)] that the ratio D/D_{LB} monotonically decreases with increasing number density of the scatterers but does not show a critical density at which the diffusion constant vanishes. Computer simulation, however, shows that the critical density does exist, at least in two dimensions. The work of Götze, Leutheusser, and Yip,[17] and later our own,[7] shows that a greatly improved theory is obtained if the Lorentz-Boltzmann operator in the ring or repeated-ring operator is replaced by the true one-particle operator, and the resulting equations solved self-consistently. These theories do show critical densities and show considerably improved agreement with the computer simulation data compared to either ordinary ring or repeated-ring theories. Because of this, we now propose a SCRRA along these lines. When $m_1/m \gg 1$ the equations become identical to the non-self-consistent RRA. When $m_1 \simeq m$ or $m_1/m \ll 1$, we suspect that the self-consistent theory will be a great improvement.

Let us write the true equation of motion of $\vec{\Phi}(1)$ in the form

$$[z-\hat{B}(\vec{v}_1)]\vec{\Phi}(1)=\vec{v}_1\phi_0(v_1)\ , \tag{48}$$

where $\hat{B}(\vec{v}_1)$, is the exact kinetic operator. Our self-consistent approximation consists of replacing $\lambda_D(\vec{v}_1)$ in Eq. (3b) with $\hat{B}(\vec{v}_1)$. Thus the new version of Eq. (3b) becomes

$$[z+\vec{v}_1\cdot\vec{\nabla}_1+\vec{v}_2\cdot\vec{\nabla}_2-\rho\hat{B}(\vec{v}_1)-\rho\lambda_B(\vec{v}_2)-\bar{T}(12)]\vec{\theta}(12)=T(12)\vec{\Phi}(1)\phi_0(v_2)\ . \tag{49}$$

We now formally solve Eq. (49) for $\vec{\theta}(12)$ and substitute the result into Eq. (3a). Comparison of this equation with Eq. (48) gives

$$\hat{B}(\vec{v}_1)\simeq\lambda_D(\vec{v}_1)+\int d\vec{r}_2 d\vec{v}_2\bar{T}(12)[z+\vec{v}_1\cdot\vec{\nabla}_1+\vec{v}_2\cdot\vec{\nabla}_2-\hat{B}(\vec{v}_1)-\rho\lambda_\beta(\vec{v}_2)-\bar{T}(12)]^{-1}T(12)\phi_0(v_2)\ . \tag{50}$$

This is our approximation for the operator $\hat{B}(\vec{v}_1)$. In order to discover what dynamical events are taken into account by the approximation we can express $\hat{B}(\vec{v}_1)$ as a power series in ρ. This is done by expanding the inverse operator in Eq. (50) about the free-streaming term and equating powers of the density. This procedure is discussed in the Lorentz-gas limit in more detail in Ref. 7.

In order to obtain numerical solutions to the coupled equations (48), (3a), and (49), we first make a BGK approximation for $\hat{B}(\vec{v}_1)$. Thus we write

$$\rho\hat{B}(\vec{v}_1)f(\vec{v}_1)\simeq-\nu(z)\left[f(\vec{v}_1)-\phi_0(\vec{v}_1)\int d\vec{v}\,'_1 f(\vec{v}\,'_1)\right] \tag{51}$$

for arbitrary $f(\vec{v}_1)$. Using this approximation in Eq. (48) yields the expression for $C(z)$ given in Eq. (41). Plausibility arguments for the accuracy of the BGK approximation are presented in Ref. 11. Once we have made this simplification, we may employ exactly the same variational procedure as discussed previously, summarized in Eqs. (38) and (39), except that ν_D in the functional K should be replaced by $\nu(z)$. If we follow the previous sections and choose the trial function $\vec{\Phi}(1)$ to be that given by Eq. (40), then the working equation becomes identical to Eq. (42), except that the K functional now involves $\nu(z)$.

In order to obtain numerical results, therefore, we took the same trial functions as given in Eqs. (44a)–(44c) and then solved the modified Eq. (42) for ν by iteration. The results of this procedure, for ν/ν_D with $m_1/m=1$, are shown plotted in Fig. 5. The ordinary RRA results are in Fig. 3. Clearly, the self-consistent theory shifts the peak to smaller values of a_1 and makes it higher. This increase of peak height is not unexpected, because in the Lorentz-gas limit the self-consistent theory predicts ν/ν_D to rise much faster than predicted by the RRA. Thus as we believe the initial rise in the curves reflects a Lorentz-gas-like behavior, it is no surprise that the curve from the self-consistent theory goes up faster initially and thus reaches a higher value before motion of the surrounding fluid brings it down again. Because the self-consistent theory is superior to the non-self-consistent theory in the Lorentz-gas limit, we suspect that the self-consistent theory would also probably be a more accurate theory for lighter tagged particles.

The main qualitative conclusion to be drawn from the calculations presented in the figures is that the variation of D/D_{LB} with a_1/a is a very sensitive function of the size and mass ratios, increasing or decreasing, sharply or mildly, depending on circumstances. Insofar as, to our knowledge, almost nothing is known in this area for non-Brownian particles, we are eager to compare the theory to real or computer experiments. The only relevant "experiments" which we have been able to locate are those of Alder *et al.*[12] These are, unfortunately, carried out at too high a bath density for the SCRRA to be trusted. The lowest bath density that they studied, equal to $\frac{1}{3}$ times the close-packed density, gives a value for a/l of 5.9. Clearly, this ratio is far too high for the Boltzmann equation to give an accurate description of the bath, and therefore the accuracy of the SCRRA at this density is suspect. Nevertheless, we are unaware of any other data, and one might hope that the theory will at least reproduce the correct trends. We present the results in Table I, where r_1 and r are the radii of the tagged particle and fluid particle, respectively. The simulation results are given in the form D/D_E, where D_E is the Enskog diffusion constant which differs from D_B by a factor of the radial distribution function at contact. For the bath density considered this factor is by no means negligible, being approximately equal to 2 for equal radii. Alder *et al.* show, however, that it is only a weak function of the ratio r_1/r, and as we are only looking for trends, not quantitative agreement, we do not think it inconsistent to compare the simulation value of D/D_E with our calculated values of D/D_{LB}.

The general results of the simulation are that for equal masses, D/D_E increases, whereas when the tagged particle is much lighter than the bath particle, D/D_E decreases as r_1/r increases. Both the RRA and the SCRRA reproduce this trend though the SCRRA seems somewhat more quantitatively

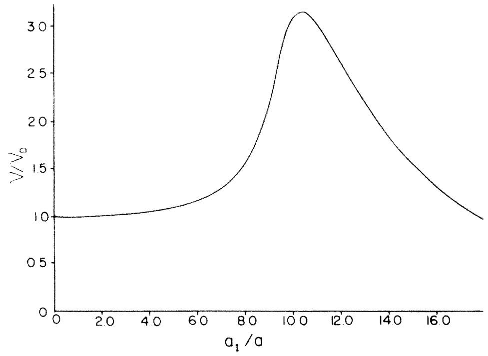

FIG. 5. Plot of ν/ν_D vs a_1/a for unit mass ratio in the self-consistent theory.

TABLE I. Mass- and size-ratio dependence of D as calculated from theory and the molecular-dynamics (MD) simulation of Alder and Alley (Ref. 12) for a bath density of $\frac{1}{3}$ times the close-packed density. Numbers in parentheses are Alder and Alley's estimates of what should be added to D/D_E to correct for "long-time tails."

m_1/m	r_1/r	$(D/D_E)_{\mathrm{MD}}$	$(D/D_{\mathrm{LB}})_{\mathrm{RRA}}$	$(D/D_{\mathrm{LB}})_{\mathrm{SCRRA}}$
1	0.25	1.09(0.04)	1.23	1.21
	0.5	1.14(0.08)	1.34	1.31
	0.75	1.15(0.12)	1.50	1.41
	1.0	1.16(0.17)	1.64	1.53
1/10	0.25	1.04(0.02)	0.90	
	0.5	0.95(0.04)	0.87	
	0.75	0.86(0.05)	0.84	
	1.0	0.75(0.07)	0.81	
1/100	0.25	1.00(0.00)	0.86	
	0.5	0.77(0.02)	0.79	
	0.75	0.56(0.02)	0.70	
	1.0	0.37(0.02)	0.60	
1/5625	0.25	1.03(0.00)	0.87	0.85
	0.5	0.75(0.00)	0.79	0.73
	0.75	0.38(0.00)	0.69	0.52
	1.0	0.19(0.00)	0.59	0.13

accurate. At this density the plot of v/v_D looks more like the curves shown in Fig. 3, showing a maximum before decreasing once again. Thus the theory would predict that if the simulation were to be carried out at a low-mass ratio with larger values of r_1/r, then the value of D/D_E would start to rise up again for large tagged particles. So, even though we are pushing the theory beyond the regime where we believe it, it is in fact reproducing the results of the simulation; we are not aware of any similarly successful theory. It seems worth pointing out that purely hydrodynamic theories have[18] been surprisingly successful in describing the motion of a tagged member of a pure liquid; the reason for this remains a mystery. Nevertheless, our finding that, for $m = m_1$, the plot of v/v_D vs r_1/r looks "Brownian" is consistent with the wide utility of hydrodynamic theories, since they are most plausible for Brownian particles.

In summary, we have shown how to treat the transition from high to low Knudsen number in diffusion of a massive particle. This has been done before for the drag, but not for D directly, and thus our theory automatically incorporates Einstein's law. More interestingly, we have determined the size-ratio dependence of D/D_{LB}, a function of mass ratio, which, so far as we know, is completely new. We would very much like to find other real experiments or simulations on which to test the theory.

ACKNOWLEDGMENT

This work has been supported by National Science Foundation Grant No. CHE-81-11422. One of us (T.K.) acknowledges support by the Dreyfus Foundation.

---

[1] M. H. Ernst and J. R. Dorfman, Physica (Utrecht) 61, 157 (1972).
[2] J. R. Dorfman, in *Fundamental Problems in Statistical Mechanics*, edited by E. G. Cohen (North-Holland, Amsterdam, 1975), Vol. III.
[3] (a) J. R. Dorfman, H. Van Beijeren, and C. F. McClure, Arch. Mech. 28, 333 (1976); (b) H. Van Beijeren and J. R. Dorfman, J. Stat. Phys. 23, 335 (1980); 23, 443 (1980).
[4] R. I. Cukier, R. Kapral, J. R. Lebenhaft, and J. R. Mehaffey, J. Chem. Phys. 73, 5244 (1980).
[5] J. Mercer and T. Keyes, J. Stat. Phys. (in press).
[6] T. Morita (private communication).
[7] A. J. Masters and T. Keyes, Phys. Rev. A 26, 2129 (1982).
[8] A. J. Masters and T. Keyes, Phys. Rev. A 25, 1010

(1982).

[9] C. Cercignani, *Theory and Application of the Boltzmann Equation* (Scottish Academic, Glasgow, 1975).

[10] C. Cercignani and C. D. Pagani, Phys. Fluids 11, 1395 (1968); C. Cercignani, C. D. Pagani, and P. Bassanini, *ibid.* 11, 1399 (1968).

[11] P. F. Bhatnagar, E. P. Gross, and M. Krook, Phys. Rev. 94, 511 (1954).

[12] B. J. Alder, W. E. Alley, and J. H. Dymond, J. Chem. Phys. 61, 1415 (1974); B. J. Alder and W. E. Alley, J. Stat. Phys. 19, 341 (1978).

[13] M. H. Ernst, J. R. Dorfman, H. R. Hoegy, and J. M. J. Van Leeuwen, Physica (Utrecht) 38, 35 (1968).

[14] S. Chapman and T. G. Cowling, *The Mathematical Theory of Non-uniform Gases,* 3rd ed. (Cambridge University Press, London, 1970).

[15] P. Résibois and M. DeLeener, *Classical Kinetic Theory of Fluids* (Wiley, New York, 1977).

[16] M. J. Lindenfeld, J. Chem. Phys. 73, 5817 (1980).

[17] W. Götze, E. Leutheusser, and S. Yip, Phys. Rev. A 23, 2634 (1981); 24, 1008 (1981); 25, 533 (1982).

[18] B. Alder, D. Gass, and T. Wainwright, J. Chem. Phys. 53, 3813 (1970).